# Standoff Acoustic Laser Technique to Locate Buried Land Mines

Robert W. Haupt and Kenneth D. Rolt

■ **The worldwide proliferation of land mines leads to thousands of civilian casualties each year and threatens military forces who patrol hostile territories. To reduce these casualties, military and humanitarian organizations seek methods to detect the large variety of mines being deployed. Many mine detection systems currently under development can detect only metal or a specific mine feature, have limited standoff range, or are impractical for field operations. A promising approach uses acoustic waves to induce mechanical vibrations in both plastic and metal mines. The vibration field above these mines can then be measured remotely with a laser Doppler vibrometer. This article describes a method to advance acoustic land-mine detection by increasing standoff range from the minefield and by developing a more practical lightweight system. We take a novel approach to excite mines by using a parametric acoustic array (PAA) source to transmit a highly directive sound beam from a safe distance. We discuss the standoff system concept, the process of PAA wave generation, and the coupling of acoustic waves to the ground to excite mines. A proof-of-concept system, built at Lincoln Laboratory, deploys a commercial PAA and a commercial laser vibrometer. We tested the system at a land-mine facility and measured distinct vibration signatures from buried anti-personnel mines. The overall concept shows promise. The PAA tested in these experiments, however, was developed for home entertainment and has marginal power for land-mine detection, even at close range. A system suitable for standoff detection requires more acoustic power and substantial modification. We estimate that power gains up to 50 dB may be achievable, and we discuss alternatives to the commercial PAA design.**

THE PROLIFERATION OF LAND MINES throughout the world has become an enormous problem for both civilian populations and military personnel. An estimated sixty to seventy million land mines are in place in seventy countries; these mines kill or maim 26,000 people each year [1]. All too often these casualties occur to those noncombatants who unknowingly encounter an uncleared minefield well after the war in their country has ended. Most of these casualties are civilians, of which about half are children under the age of sixteen. The United States is currently involved in several foreign conflicts where troops are in constant danger from land mines and mine-like traps set along roads and in fields. Fatalities and injuries are reported almost daily. The current crises in Iraq, Afghanistan, and other countries, and the ongoing need to remediate minefields from previous conflicts, clearly motivate the development of reliable methods that quickly locate land mines, unexploded ordnance, and other mine-like targets.
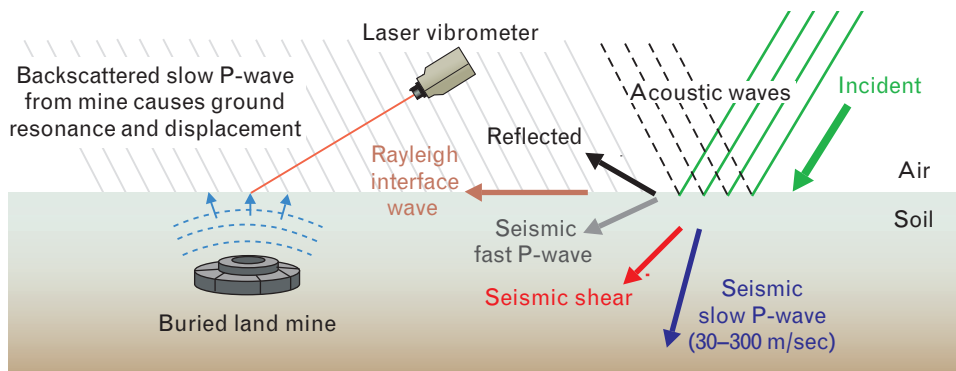
FIGURE 1. Acoustic-to-seismic wave-coupling approach to detect buried land mines. Acoustic sound waves penetrate the soil surface to generate seismic waves within the soil. These seismic waves cause the mine to vibrate and resonate, producing a displacement velocity field at the ground surface above the mine. This displacement can be measured by a laser vibrometer or UHF radar.

Most land-mine detection relies on careful searches of mined areas with handheld metal detectors. Consequently, mine detection and removal are dangerous and labor-intensive activities. Furthermore, plastic and non-metallic mines have been developed as a countermeasure to metal detectors, and are now used on a global scale. Because of the small contrasts in electrical properties between soil and nonmetallic mines, the most widely used methods of electromagnetic induction (handheld metal detectors) and ground-penetrating radar are not always effective. In contrast, the mechanical properties of plastic and metal mines vary significantly from those of soil, which may make acoustic excitation a more reliable mechanism to detect mines. Acoustic-to-seismic techniques are currently being researched and have shown promise as a method of detecting mines made of many materials buried in a variety of soils [2–8].

These techniques rely on the permeability of soil and the penetration of controlled sound waves into the first few inches of soil. The penetrating sound waves generate a series of seismic waves within the soil, including seismic slow P-waves that can have speeds slower than sound in air and wavelengths close to the size of mines. These slow P-waves can cause land mines to vibrate and resonate differently from the surrounding soil, which produces an anomalous displacement velocity field at the ground surface just above the mine. This vibration can literally lift and drop the thin cover of soil above the mine. This soil motion can be measured spatially by a laser Doppler vibrometer [2–6] or by a UHF radar [7, 8], and can be used to map the mine location. Figure

1 illustrates the acoustic-to-seismic approach to mine detection.

The acoustic-to-seismic method is particularly attractive because it provides a high probability of detection with a low false-alarm rate [9]. The low false-alarm rate can be attributed to the difference in the mechanical compliance of the land mine versus that of soil, rocks, sticks, and other buried objects. The compliance is defined as the strain response (change in object shape) for a given stress (load imposed by an acoustic wave), and can also be thought of as the acoustical equivalent of electrical capacitance [10]. Mine membranes and plungers are designed to depress and detonate the mine when a person or vehicle encounters the mine. As a consequence, these membranes and plungers are highly compliant and can vibrate in response to sound, causing the mine to act as a passive radiator when excited by the appropriate acoustic frequencies. Rocks, sticks, bricks, and other solid objects buried in the soil are relatively stiff, or noncompliant, and produce much smaller vibrations than mines.

Challenge of Standoff Detection

A standoff distance of thirty meters or more between the detection system and the mine provides a safety zone critical to the operators in the event a mine detonates. In addition, search speed, system size and weight, and covertness are key factors that are highly desirable for an operationally feasible system that may be used by the military. Delivering the acoustic power required to excite buried mines at a distance of thirty meters is

a difficult challenge. A single loudspeaker is unlikely to deliver the needed power at this range. An array of speakers could achieve the acoustic power requirements, but the massive size and weight of the array would be impractical for operational use. In addition, the sound level close to an array of speakers would be well above the hearing threshold of pain, thus reducing safety and comfort for the operator and others nearby.

A parametric acoustic array (PAA) source may provide a practical means to deliver the necessary level of acoustic power in air to the mine while minimizing system size and weight, and reducing the sound level imposed on personnel close to the source. A PAA differs from a loudspeaker in the manner in which sound is created. The loudspeaker radiates audible sound directly from a diaphragm that vibrates at some frequency, and it is the vibration of the diaphragm that emits sound at the same frequency into the air. The radiation pattern of a loudspeaker is typically broad to cover a wide listening area. The PAA, in contrast, has two sources of sound. One source is high frequency, and is generated directly from one or more high-frequency transducers. The other source is low frequency, and is generated from nonlinear effects in the volume of air in front of the transducers.

For our purposes, the PAA exploits the nonlinearity of the air to generate audible frequencies from inaudible ultrasound, resulting in an extremely directive acoustical source. Commercial PAAs developed for loudspeaker applications [11] can transmit audible sound over a distance of a hundred meters, and weigh only a few pounds. The critical question is whether a PAA can deliver the acoustic power and bandwidth required to excite mines at a reasonable standoff range, thus enabling mine detection. This article examines the potential of using a PAA and a commercial laser vibrometer to detect buried land mines at range.

Acoustic-to-Seismic Coupling

When acoustic waves come in contact with the ground, most of the energy reflects back into the air. A small percentage of these waves, however, couples to the ground, causing ground motion that transmits a series of seismic waves. These seismic waves consist of a surface wave (the Rayleigh wave) that travels at the air/soil interface, and body waves that travel in the soil (a shear wave and two compressional waves). The Rayleigh wave, the shear wave, and one of the compressional waves, called the *fast P-wave*, propagate within the solid granular matrix in soil at speeds typically greater than several hundred meters per second. At these speeds, and over much of the audible bandwidth, the associated seismic wavelengths are considerably larger than land-mine dimensions. The second compressional wave, called the *slow P-wave*, exhibits speeds slower than the other seismic waves and is controlled by the void space in soil (which determines porosity and permeability) and the fluid content (both air and water) in soil pores. Some slow P-waves are observed to travel significantly more slowly than the speed of sound in air, thus producing wavelengths at the scale of the size of land mines.

Seismic Wave Characteristics

The equations describing acoustic-to-seismic wave coupling and wave propagation in soil are mathematically complicated, and are not discussed in detail here. A more detailed description can be obtained from M.A. Biot, who developed the theory of elastic wave propagation in porous media [12]. Y.F. Sun also developed complex expressions, derived from Biot's fundamental equations, to determine the fast and slow P-waves and the shear-wave velocities in porous media [13]. Equations 1 through 3 describe the velocity dependence on the mechanical properties of soil and on the wave propagation frequency:
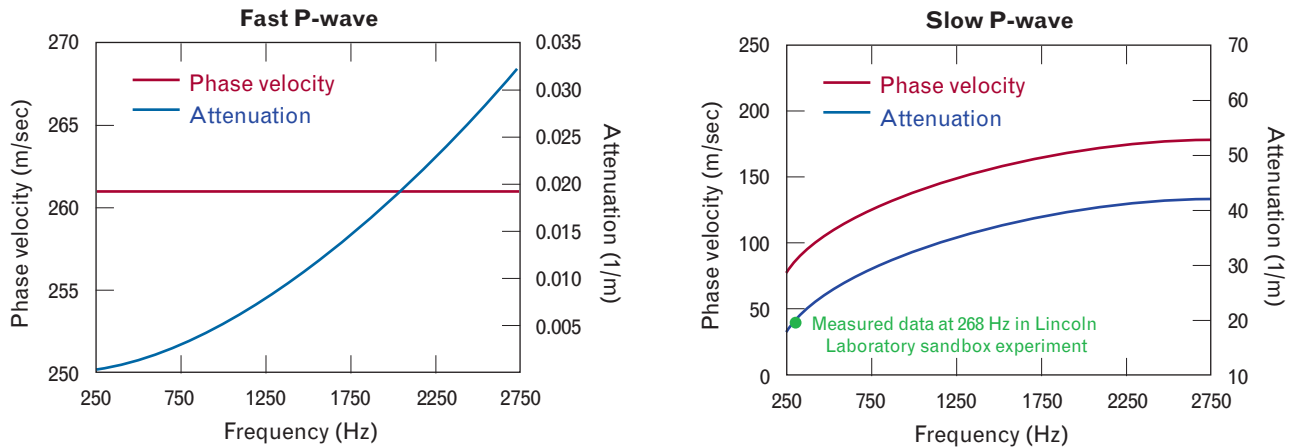
$$V_P(f)\,fast = \left(\frac{\dfrac{1}{C_M(f)} + \dfrac{4G(f)}{3}}{\rho_M + \rho_F} \right)^{1/2}, \qquad (1)$$

$$V_P(f)\,slow = \left(\frac{\dfrac{1}{C_F(f)}}{\rho_M + \rho_F} \right)^{1/2}, \qquad (2)$$

and

$$V_S(f) = \left(\frac{G(f)}{\rho_M + \rho_F} \right)^{1/2}. \qquad (3)$$

The quantities C_M and C_F are the soil grain matrix and

FIGURE 2. Comparison of modeled propagation characteristics of fast and slow seismic compressional waves (P-waves) in soil. The fast P-wave exhibits a constant phase velocity and a small increase in attenuation with increasing frequency. The slow P-wave exhibits a phase velocity and attenuation that increase with frequency. For the slow P-waves, the increased attenuation is attributed to the effects of fluid drag that increases in soil pores as frequency increases.

soil pore fluid compressibilities, ρ_M and ρ_F are the soil grain matrix and soil pore fluid densities, and f is the frequency. The quantity G is the soil rigidity, or shear modulus, which can support shear stresses only in a solid. Thus shear waves do not propagate in a fluid. Equations 1 and 3 are forms of the standard equations of the fast P-wave and the shear wave [10]. Equation 2 is based on a mixture model we developed to explain simply the characteristics of the slow P-wave.

Figure 2 compares the modeled propagation characteristics of fast and slow P-waves in soil, as shown by J.M. Sabatier [14]. The fast P-wave exhibits a constant phase velocity and a small increase in attenuation with increasing frequency. These effects are attributed to the non-dispersive nature of the solid portion of the soil matrix, which easily transmits elastic waves over the audible band with low loss. In comparison, the slow P-wave disperses with frequency and exhibits a phase velocity and attenuation that each increase with frequency. Compressibility of the fluid (air and water) contained in the soil pores retards the wave speed. As the frequency of the wave increases, viscous forces stiffen the fluid, thus decreasing its compressibility and increasing the wave velocity. Table 1 summarizes the predicted seismic compressional wavelengths of fast and slow P-waves. Even at lower seismic frequencies, the slow P-wave has wavelengths approaching the size of land mines, which are on the order of 5 to 10 cm for anti-personnel mines and up to 30 cm for anti-tank mines.

Seismic Wave Attenuation

The attenuation is orders of magnitude larger for the slow P-wave than for the fast P-wave. The increased attenuation is attributed to the work required by the slow P-wave to oscillate and drag fluid in the soil pores, thus expending wave energy. The larger number of wave cycles, or oscillations, of higher-frequency waves expends more energy per unit distance than lower-frequency waves, and gives rise to the increased attenuation with increasing frequency.

Soil permeability causes dispersion that allows lower-frequency waves to penetrate more deeply into soil while higher-frequency waves attenuate rapidly. The dispersive nature of soil to acoustic-to-seismic coupling was observed in sandbox measurements conducted at Lincoln Laboratory. Figure 3 shows the results of these

Table 1. Predicted Seismic Compressional Wavelengths

| Frequency (Hz)	Fast P-wave wavelength (cm)	Slow P-wave wavelength (cm)
250	104	32
1000	26	13
2000	13	8
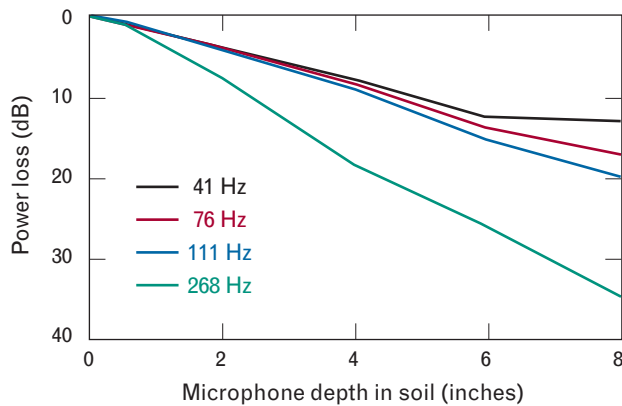
FIGURE 3. Measured one-way acoustic power loss in soil as a function of microphone depth and tone frequency. Attenuation is less than 5 dB at shallow depths, but significantly greater as the depth increases, particularly at higher frequencies. Mines are typically placed between one and three inches below the soil surface. Attenuation makes the deeper mines more difficult to detect.

experiments. A microphone was buried at different depths in dry sand to measure acoustic tones played by a loudspeaker in the air above the sand. Each tone played by the loudspeaker had the same amplitude and was broadcast for the same time duration. The microphone depths were similar to those which might be encountered in a minefield. Anti-personnel mines are typically buried less than one inch deep, and the observed one-way propagation power loss is less than 5 dB for

frequencies below 300 Hz. Anti-tank mines, however, are typically buried three inches deep, and at that depth the observed one-way propagation loss approaches 20 dB at a tone frequency of 268 Hz. This power loss at 268 Hz agrees with the modeled slow P-wave calculations, as shown by the green dot in Figure 2.

Impedance Contrast

Although the fast P-wave exhibits a smaller attenuation over frequency compared to the slow P-wave, the fast P-wave has significant limitations in mine detection. These limitations depend on the impedance contrast, which is the difference in mechanical properties between soil and the mine, and which control backscatter and mine vibration. Mechanical properties such as the density and elastic moduli of the solid matrix of the soil are comparable to those of plastic and metal mines, which results in a small impedance contrast. Thus the backscattered return off a mine would be small for fast P-waves at any frequency, which negates any advantage the fast P-wave might have to excite buried mines. Figure 4 illustrates this phenomenon; the dashed lines in the graph on the left show the notional impedance contrast between soil and a mine as a function of depth. The solid lines shows the impedance contrast due to soil compaction with depth. Clearly, the slow P-wave shows a significantly larger peak in impedance contrast at the mine location.
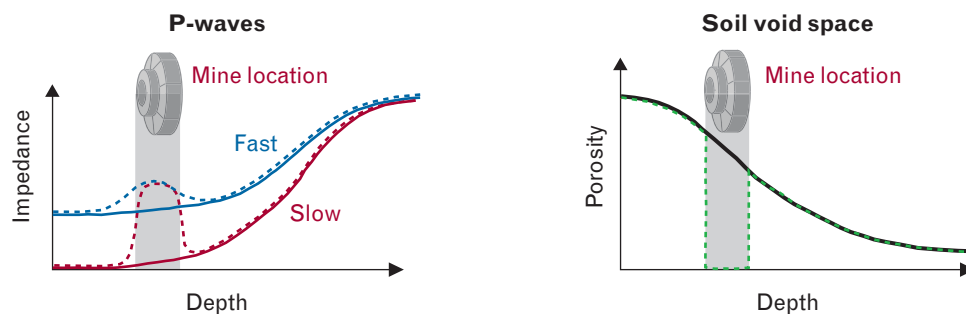
FIGURE 4. Comparison of characteristics of fast and slow P-waves in soil. The dashed lines in the graph on the left show the normalized impedance contrast between the soil and a buried mine as a function of depth for fast and slow P-waves. The solid lines show the impedance contrast caused by soil compaction. The limited contrast differences between the soil and a buried mine restrict the ability of fast P-waves to excite mines. For slow P-waves, the significant contrast differences in impedance between the soil and a mine can be exploited for more effective detection. The solid line in the graph on the right shows how porosity of the soil decreases with depth, but the porosity of a mine is essentially zero, as shown by the dashed line, which is responsible for a strong impedance contrast that greatly affects slow wave propagation and can lead to detection.

The impedance contrast of the slow P-wave depends on the soil porosity, which is a measure of the void space in soil. Because of soil compaction, porosity in soil decreases with depth, as shown by the solid line in the graph on the right in Figure 4. The porosity of soil can vary from nearly zero to almost 90%, while the porosity of a metal or plastic mine is essentially zero, as shown by the dashed line. This difference in porosity produces a large impedance contrast in the slow P-wave between the mine and soil, which causes the slow P-wave to backscatter and promotes vibration of the mine.

While the effects of permeability (the interconnected pore space in soil) rapidly attenuate the energy of the slow P-wave, reasonable propagation still occurs within the top several inches of soil where most anti-personnel and anti-tank mines are buried. Acoustic-to-seismic wave coupling is most effective in exciting anti-personnel mines within an inch of the soil surface, where higher frequency wavelengths can be used, and propagation power losses in the slow P-wave are minimized.

Standoff Acoustic-to-Seismic Land-Mine Detection System

The standoff distance at which a mine can be detected depends on the generated power of the acoustic source and the sensitivity of the laser vibrometer or radar vibration sensor. Current proof-of-concept systems operate within a few meters from the mine. Sabatier, N. Xiang, D.M. Donskoy, and M.S. Korman [2–6] have demonstrated the acoustic-to-seismic technique to detect and map buried mines with a system that employs one or two large loudspeakers and an acoustically isolated scanning laser vibrometer. Both source and sensor are down-looking on the order of one meter above the mine target. Although these experiments show that the technique has merit as a mine detection and mapping tool, these detection systems have limited standoff range. They are also large in size and weight, and therefore may not be practical for operational deployment.

A PAA source and a laser sensor are potentially suitable for development as a standoff land-mine detection system that is operationally feasible for ground vehicle or helicopter platforms, or in a man-pack configuration. The PAA exploits the process of self-demodulation that promotes the conversion of a narrow sonic (or ultrasonic) beam to create an extremely directive lower-frequen-
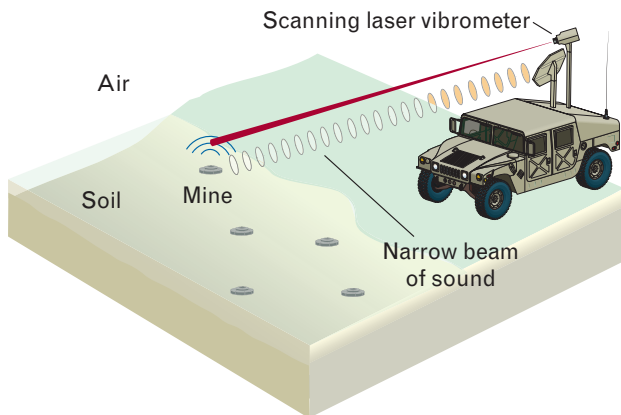
FIGURE 5. Concept of a truck-mounted standoff land-mine detection system using a directed narrow-beam parametric acoustic array (PAA) sound source and a laser-vibrometer seismic detector. The sound source penetrates the ground, causing the mine to vibrate. The laser vibrometer measures the vibrations at the ground surface.

cy sound that would otherwise require an enormous array of audible-frequency transducers or loudspeakers. It is this difference frequency that has the ability to penetrate the ground and excite the mine. The ultrasonic frequency by itself, however, attenuates too rapidly in air or in ground to excite the mine directly.

Figure 5 shows the conceptual elements of such a system. The PAA generates a directed narrow beam of sound. The sound waves couple and penetrate into the ground, causing a mine to vibrate. The laser vibrometer measures the resultant vibrations at the ground surface. The objective is to develop a system that can search for mines in an area in front of a stationary or moving vehicle, and map the locations of these mines, from a safe range of thirty meters or greater.

Parametric Acoustic Array Source

Previous PAA research has focused on applications in sonar [15] and in directive and beam-like sound in air for commercial loudspeaker systems [11, 16, 17]. In his 1963 paper, P.J. Westervelt introduced the term "parametric acoustic array" [18], and provided the mathematical framework for much of the later work in nonlinear acoustics and parametric sound sources.

The parametric acoustic array was named for its similarity to the parametric amplifier, which combines two RF signals, a pump and an input, together with nonlinear mixing to form a modulation product. The

modulation product is an RF wave that is translated (up or down) in frequency from the pump frequency. The pump signal provides the input energy for the amplifier and is modulated in amplitude by the input signal.

The PAA combines pump acoustical signals, typically ultrasonic, at two different frequencies, ω_1 and ω_2, to form a modulation envelope. The modulation envelope undergoes natural mixing to generate new frequency components in the modulation product because of the nonlinear behavior of the fluid; this process is called self-demodulation. The useful part of the modulation product for the PAA is always the difference frequency ω_d, where $\omega_d = |\omega_1 - \omega_2|$; the signal amplitude at this difference frequency grows progressively with propagation. Full or partial amplitude modulation of a single-tone pump acoustic wave can also produce a modulation product.

The PAA is an end-fire-steered, continuously distributed volume of difference-frequency sources created during the self-demodulation process. This volume is confined within the main-radiation-axis near field of the pump. The near-field difference-frequency sources are cumulative in strength. They have amplitudes that grow progressively with range from the pump source, and can be thought of as being coherently stimulated in a traveling-wave end-fire sense by the pump carrier. Hence the PAA borrows the terminology, and in some sense the physics, of the parametric amplifier in RF practice, end-fire arrays from antenna theory, and the pump and coherent stimulation found in lasers.

Linear versus Nonlinear Acoustics

Generally speaking, all acoustic waves are nonlinear. However, in more common applications of acoustics, such as in speech, nonlinear effects are negligible. Nonlinear effects become significant when the initial sound is very loud. This is illustrated in the nonlinear acoustic wave equation for fluids (i.e., for gases and liquids),

$$\frac{\partial^2 p'}{\partial t^2} = c_o^{\ 2}(1 + \beta \frac{v'}{c_o})^2 \frac{\partial^2 p'}{\partial x^2}. \tag{4}$$

Equation 4 is a simplified form of a one-dimensional nonlinear acoustic wave equation, in an *x-t* space-time coordinate system, where p' is the acoustic pressure, c_o is the ambient sound speed, v' is the acoustic particle velocity, and β is the coefficient of nonlinearity for the fluid. The nonlinearity arises due to the pressure-density dependence of the fluid. The ratio of v'/c_o is called the *acoustic Mach number*. Because the wave speed c_o is a constant, the wave equation becomes linear as $\beta v'/c_o$ approaches zero. The linear wave equation satisfies superposition and homogeneity, which results in undistorted wave motion. When $\beta v'/c_o$ is significantly larger than zero, the effective wave speed becomes $c_o + \beta v'$, which—depending on the sign and strength of v'—leads to cumulative distortion during wave propagation.

Figure 6 illustrates this cumulative distortion by showing a single cycle of a sine wave traveling to the right. The points *a* and *b* on the *x*-axis represent the locations where the magnitude of the particle velocity v'
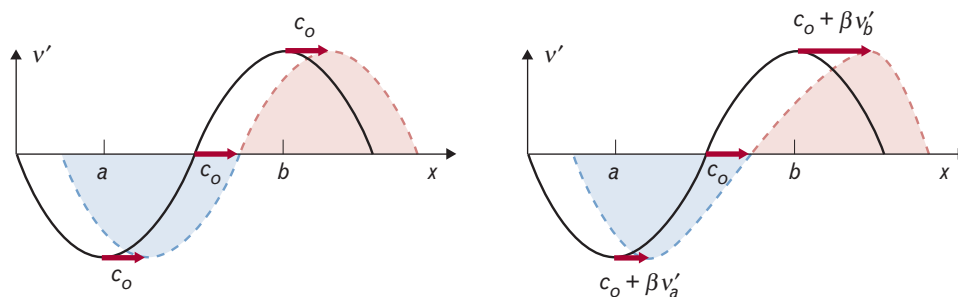
FIGURE 6. One-dimensional example of linear (left) and nonlinear (right) progressive acoustic waves. The positions *a* and *b* indicate the locations of the peaks in fluid particle velocity at an initial time. For very small values of the acoustic Mach number v'/c_o, where v' is the acoustic particle velocity and c_o is the ambient sound speed, the acoustic wave equation becomes linear, resulting in uniform wave motion. As the acoustic Mach number increases, cumulative nonlinear distortion alters the wave motion, resulting in a sawtooth shape. Compression regions (shown in red) and rarefaction regions (shown in blue) are determined by the amplitude and sign of the phase speed $c_o + \beta v'$, where β is the coefficient of nonlinearity for the fluid.
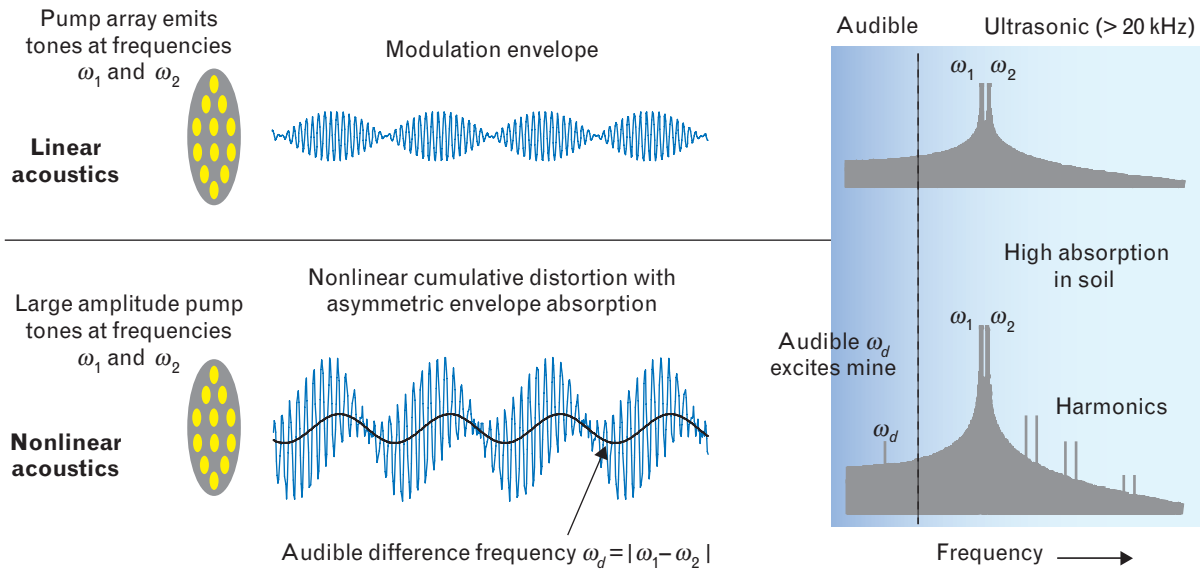
FIGURE 7. The self-demodulation process forms an audible difference frequency ω_d, which is used to detect land mines. An acoustic source radiates two pump tones at nonaudible frequencies ω_1 and ω_2, forming a modulation envelope. For linear acoustics (i.e., low sound levels), the frequency spectrum at all distances yields only the two initial pump tones. For nonlinear acoustics (i.e., loud sound levels), other tones and harmonics appear in the spectrum. The acoustic field near the source shows a progressive increase in the strength of the audible difference-frequency signal ω_d with range. Far from the sound source, the natural low-pass attenuation of the air reduces the high-frequency pump tones and the associated harmonics, leaving only the audible difference-frequency signal.

is a maximum. For linear acoustics, the effective wave speed for these locations, as well as for the three zero crossings shown, is c_o. At a time Δt later, the peaks have traveled coherently to new locations, preserving the original wave shape, as shown in the graph on the left in Figure 6.

For nonlinear acoustics, the sine wave distorts during travel into a sawtooth shape, as a result of the amplitude- and sign-dependent phase speed $c_o + \beta v'$. Positive values of v' result in compression of the wave (shown in red in the figure), while negative values of v' result in rarefaction (shown in blue). In other words, compressions travel faster than c_o while rarefactions travel more slowly than c_o, and wave distortion is always the result. The dashed line in the graph on the right in Figure 6 illustrates this sawtooth distortion. Common examples of sounds produced by nonlinear acoustics include thunder, sonic booms, and gunfire.

Self-Demodulation Process

For the PAA, the waveform is clearly more complicated than a single cycle of a sine wave, but the amplitude-dependent distortion effects are the same. As illustrated

in Figure 7, an acoustic source radiates two pump tones at frequencies ω_1 and ω_2. These tones form the modulation envelope that depicts beating waves traveling away from the source. The tones decrease symmetrically in amplitude via absorption along the x-axis as the wave propagates. In linear acoustics, for small sound levels ($\beta v'/c_o \ll 1$), the measured spectrum at any location in the sound field (near or far) shows the two pump tones at ω_1 and ω_2, as illustrated in the frequency spectrum in the upper part of Figure 7.

In nonlinear acoustics, where the pump amplitudes are large, the acoustic field near the source shows a progressive increase in the strength of the difference-frequency signal with range (as limited by Westervelt's equation). As shown previously in the example of nonlinear behavior of a single sine wave, sawtooth-shaped waves appear, but the modulation envelope pre-warps the waves first, as shown in the lower part of Figure 7. The pre-warping is followed by wave distortion, which either sharpens or smooths each part of the wave in an unequal manner, depending on the sign of the wave (compression, rarefaction) and on the location (rising, or falling, part of the envelope). This combination leads

to asymmetrical absorption of the wave envelope, and results in the difference-frequency modulation product. Asymmetric nonlinear effects on acoustic absorption and the modulation envelope are discussed in more detail by K.D. Rolt [19]. Measured far from the sound source, natural low-pass filtering attenuation in air reduces the high frequency levels of ω_1 and ω_2 and their harmonics ($2\omega_1$, $2\omega_2$, …) so that only the lower difference frequency ω_d remains. The difference frequency and the higher harmonics are illustrated in the frequency spectrum in the lower part of Figure 7.

End-Fire Volumetric Array

The PAA generates the audible difference-frequency sound in an end-fire volumetric array. This end-fire array results from the coherent stimulation of the difference-frequency wave as it propagates and builds in amplitude. Thus the volume of air in front of the PAA can be thought of as a virtual loudspeaker. The upper part of Figure 8 depicts the end-fire volumetric array, where ultrasonic transducers form and maintain the acoustic beam. The pump modulation envelope is generated in a narrow beam within the near field of the transducer array. As the modulation envelope propagates, a nonlinear interaction occurs with air, causing acoustic self-demodulation. An audible difference frequency is produced and, under optimum design conditions, the narrow beam shape of the pump is maintained. Within the near field, the nonlinear reaction builds to a range where the difference-frequency sound pressure achieves a maximum. When the modulation envelope reaches the end of the near field of the transducer array, it attenuates rapidly as a result of geometric spreading, and the nonlinear self-demodulation effectively ends. The audible difference frequency, however, generated in the near field and generated as an end-fire array, continues to propagate as a linear acoustic wave. Eventually, the audible difference frequency also loses power from the effects of attenuation and geometrical spreading with distance.

The self-demodulation process of the PAA is inefficient because only a small percentage of the initial pump energy is converted to the difference-frequency wave. Typically, this loss can be on the order of 20 to 80 dB, as depicted in the graph in Figure 8. Although this loss is quite large, the PAA can convert a narrow
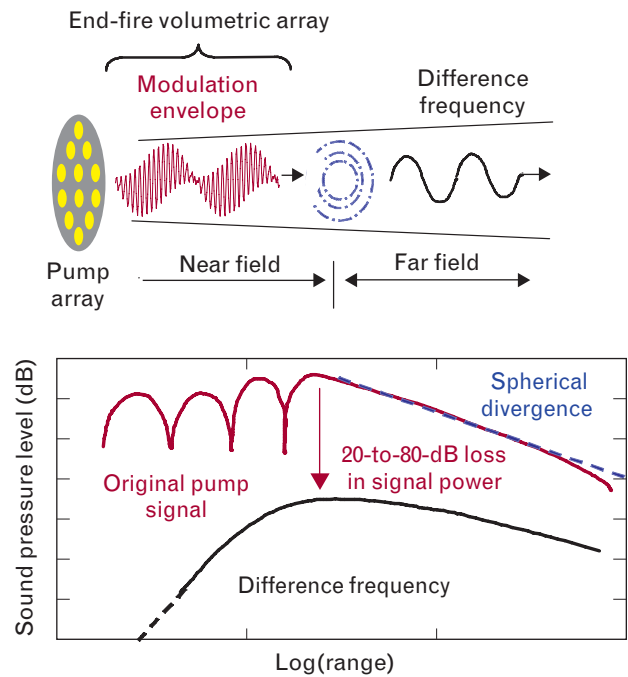
FIGURE 8. PAA source radiation, generated by an end-fire volumetric array, is created by coherent stimulation of the difference-frequency wave as it propagates and accumulates with range. Because the difference-frequency wave amplitude increases with range, the volume of air in front of the PAA is considered a virtual loudspeaker. Under optimal conditions, the end-fire volumetric array preserves the narrow signal beam of the difference-frequency wave into the far field, where it propagates as a linear acoustic wave. The graph illustrates the relative inefficiency of the PAA as a source of the difference frequency wave. The power level of the difference frequency is often 20 to 80 dB below the original pump tones, and diminishes still more in the end-fire far field because of spherical divergence and attenuation.

ultrasonic beam into an extremely directive lower-frequency sound. This conversion would otherwise require an enormous array of loudspeakers. When properly designed, a PAA can generate a difference-frequency wave that maintains the narrowness of the high-frequency pump beam at a considerable range.

Estimation of Difference-Frequency Pressure

An important artifact of the self-demodulation process is that power drops several orders of magnitude converting from the ultrasound to the audible difference frequency. Although this drop is large, it still may be possible to generate sufficient acoustic power at range to excite buried mines. The difference-frequency pressure

P_{diff} can be estimated as a function of range by using a form of the Westervelt equation shown below.

$$P_{diff} = \frac{\beta}{8\pi\sqrt{2}\rho c_o^4} \frac{P_1 P_2 \omega_d^2}{R} S_0 L, \tag{5}$$

where

$$L \approx \min\left\{\frac{1}{\alpha_i}, \frac{\sqrt{2}S_0}{\lambda_i}, \frac{3}{\beta\varepsilon k_i}\right\}. \tag{6}$$

Table 2 defines the variables used in the Westervelt equation. All of the terms in the equation are straightforward, except for the length L of the end-fire array. The value of the length L represents the range at which the pump wave amplitude becomes too weak to generate energy at the difference frequency. We write L as the minimum of three characteristic lengths—A_L, R_L, and S_L—where A_L is the pump attenuation effective distance $1/\alpha_i$, R_L is the Rayleigh distance for the pump frequencies $\sqrt{2}S_0/\lambda_i$, and S_L is the pump saturation distance $3/(\beta\varepsilon k_i)$. The saturation distance occurs when the strongest part of the wave forms a sawtooth shape, as shown in the right side of Figure 6. The pump can lose strength from ordinary sound attenuation (α_i), or from geometric spreading (propagation beyond the near field, or Rayleigh distance), or from saturation attenuation (when $\alpha_{saturation} \gg \alpha_i$). Each of these three terms is wavelength dependent, and one (the saturation distance) is pump-amplitude dependent. The varied wavelength dependence of the three parameters suggests an optimal solution for the length L, which is discussed in more detail later in this article.

Acoustic-Laser System Measurements

We built an acoustic-laser system at Lincoln Laboratory to test the potential of the PAA to excite buried land mines. The system was constructed from commercially available components, including a 24-in diameter Audio Spotlight ultrasonic transducer array (the PAA source) and processor/amplifier, both purchased from Holosonics Research Labs, Inc., and a PDV-100 laser vibrometer purchased from Polytec, Inc. An 800-W, 15-in-diameter commercial JBL, Inc., subwoofer was used as a wide-beam conventional acoustic source for comparison purposes. A sixteen-channel data-acquisition system simultaneously recorded the laser vibrometer, microphone, and geophone receivers. The system was tested and refined during a series of indoor sandbox experiments. Outdoor tests were also conducted on mock mine targets to better refine the measurement technique in preparation for measurements at a landmine facility.

The system was next used to test the potential of the PAA to excite mines *in situ* at a government land-mine facility. A variety of anti-personnel and anti-tank mines are buried at the actual depths of operation. The mines are fully configured with explosives and have been buried in place for two years. The mine firing mechanisms were removed to ensure safety and to enable access into the facility.

Acoustic-Laser System Setup

Figure 9 shows the acoustic-laser system setup at the land-mine facility and the commercial ultrasonic transducer array used to create the PAA. The transducer array and the laser vibrometer were placed three meters from the land mine; both were aimed at a down-looking angle of about 45°. Because the PAA is highly directive, a microphone was used to measure the emitted acoustic signal strength on the ground to ensure the laser measurement position was in the center of the acous-

---

Table 2. Variables in the Westervelt Equation

Properties of air

β	Coefficient of nonlinearity
ρ_o	Air density
c_o	Wave speed

Power

P_i	Pump pressure amplitude
ω_d	Difference frequency
R	Measurement range ($R > L$)

Aperture

L	End-fire array length
S_o	Pump aperture area
α_i	Pump attenuation
k_i	Pump wave number
λ_i	Pump wavelength
v'	Acoustic particle velocity
ε	Mach number (v'/c_o)
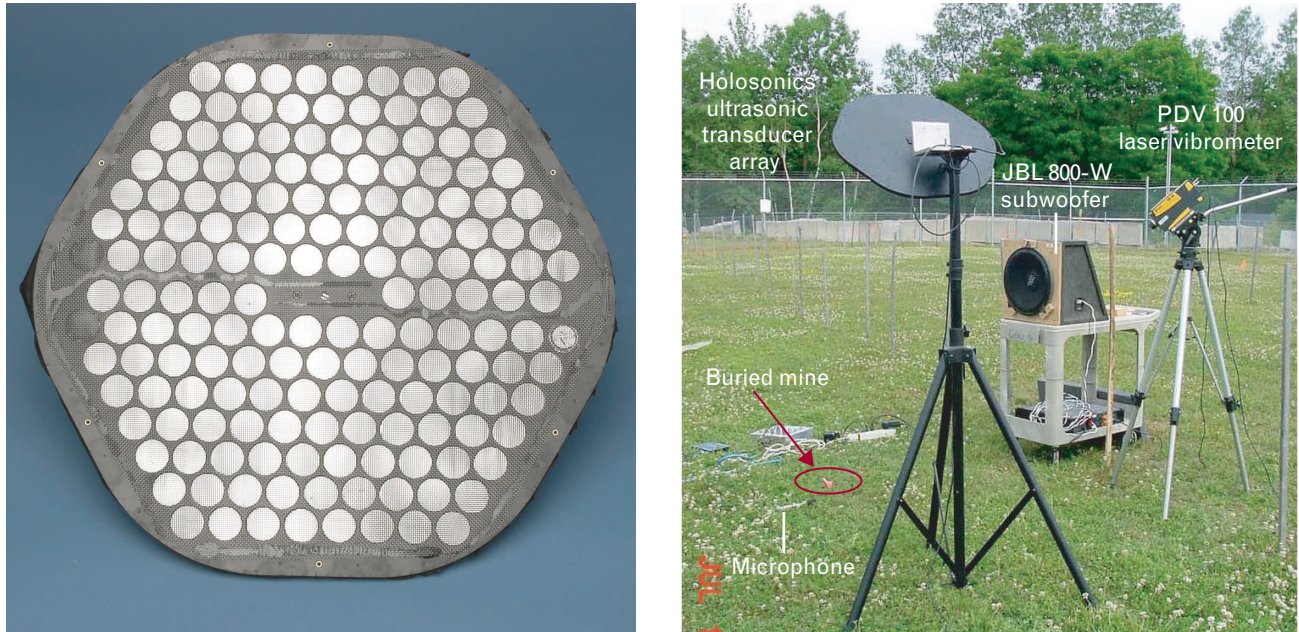
FIGURE 9. The Holosonics 162-element ultrasonic transducer array (left) and the acoustic-laser system configuration at the outdoor land-mine facility (right). The transducer array drives the PAA that directs acoustic energy toward the buried land mine, and the laser vibrometer measures the seismic displacement of the soil above the mine. The transducer array weighs four pounds, and has a maximum power of 100 dB and a maximum audible range of two hundred meters. The PDV 100 laser vibrometer has a noise floor of 0.05 μm/sec. A JBL subwoofer was used to duplicate responses found by other researchers.

tic beam. The transducer array amplifier was driven by a laptop computer with linear frequency modulated (FM) chirp functions at frequencies from 500 to 3000 Hz. The bandwidth was previously determined in outdoor experiments at Lincoln Laboratory that produced measurable responses from mock mine targets.

Laser measurements at the land-mine facility were taken in separate trials at points directly above the mine (i.e., *on* the mine) and at points adjacent to the mine position (i.e., *off* the mine). We found that using a pinhead spot size of ground glass placed on bare ground in the laser-vibrometer measurement location greatly improved the signal-to-noise ratio of the laser vibrometer and thus reduced signal integration time. This technique, which was used consistently for all measurements on and off the mine, allowed us to overcome sensitivity limitations of the laser vibrometer.

Measurements and Data Processing

Figure 9 shows the configuration of the laser vibrometer and the PAA setup. Figure 10 shows the cross-correlation time-series laser response on and off the mine, using the commercial PAA. We used the microphone as

a reference to verify and record the direct acoustic wave at the ground surface adjacent to the buried mine. Pulse compression was used to generate a short-pulse time series by cross-correlating the laser and microphone channel chirp time series for a single acoustic sweep over the chirp bandwidth. The example shows the response of a VS50 anti-personnel mine buried a half-inch deep.
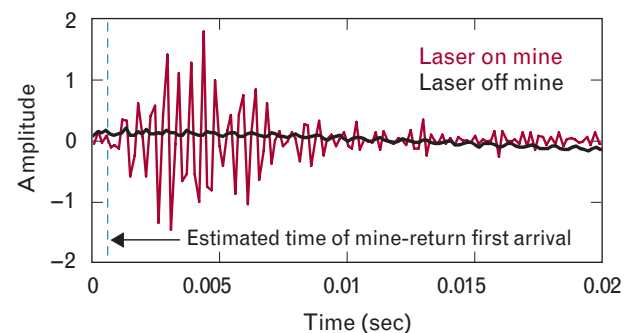
FIGURE 10. Time series measurements of a VS50 antipersonnel land mine at the outdoor land mine facility, using the commercial PAA. The signature response is clearly different when the laser vibrometer measures the movement of the soil over the land mine. The first arrival of the return can be used to estimate the depth of the mine in soil.

The time-series measurements clearly show that there is a distinct signature difference on and off the mine. Very little response is observed off the mine, while large amplitudes are observed over the mine. Also, the first break in the time-series signal over the mine, as shown in Figure 10, can be used to estimate the depth of the mine, if we have an estimate of the wave speed in soil. In a true standoff system, a microphone placed in the mine vicinity would not be practical for this measurement; however, a reference laser position could accomplish the task remotely.

Land-mine measurements were also performed by using the JBL subwoofer instead of the commercial PAA. We performed these measurements with the subwoofer to duplicate the land-mine responses found by other researchers. Sabatier and others [2–6] observed mine resonance signatures from 100 to 500 Hz for a variety of anti-tank and anti-personnel mines.
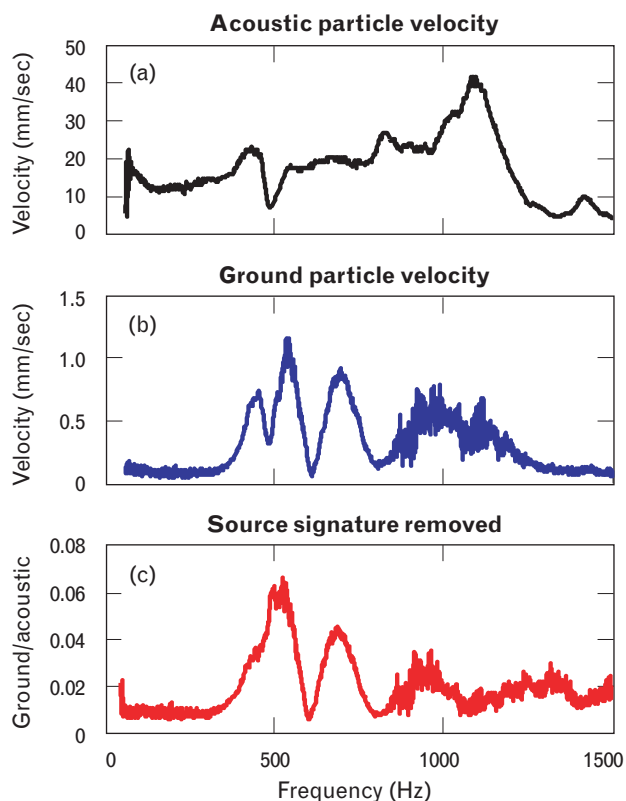

FIGURE 11. Removal of subwoofer acoustic signature from ground velocity. (a) The subwoofer signature as measured with a microphone; (b) the ground-velocity signature over the mine, as measured with the laser vibrometer; (c) the deconvolved source signature removed from the laser-vibrometer ground-velocity signature.

A consequence of using the subwoofer is that the speaker power varies with frequency over the FM chirp. The subwoofer acoustic signature was measured with the microphone on the ground surface next to the mine. Figure 11(a) shows this acoustic signature. The subwoofer exhibits a large peak at approximately 1100 Hz and a trough at 500 Hz. These fluctuations in acoustic velocity tended to affect the resonance signature observed by the laser vibrometer, as shown in Figure 11(b). The fluctuations can be removed by using deconvolution methods. This result of the deconvolution was accomplished in the frequency domain by dividing the laser signal by the microphone signal, as shown in Figure 11(c). It is important to note that the microphone has a flat spectral response in the frequency band of interest, and should not contaminate the observed direct airborne acoustic signature.

Land-Mine Signatures

Figure 12 shows the signatures for anti-tank and anti-personnel mines, which were generated by using the subwoofer. In these examples, the cart-mounted subwoofer was positioned approximately three meters from the mine, and radiated a linear FM chirp from 50 to 1500 Hz. We observed that the subwoofer power dropped dramatically above 1500 Hz, which is consistent with the manufacturer's design. Laser measurements were taken on and off the mine. Several tests were performed to observe if the subwoofer imposed vibrations (through the cart) that had a seismic influence, but none were observed. The black curves in the figure show the responses off the mine, and the red and green curves show the responses on the mine.

In all cases, the on-mine signature amplitudes were significantly larger than those off the mine. Large amplitude resonances were observed for the anti-personnel mines from 400 to 600 Hz. Smaller amplitude resonances were observed for the anti-tank mines at 150 to 400 Hz. The resonance signatures were also repeatable for the same mine on different days, and we were able to produce similar signatures for the same type of mine at other locations in the land-mine facility. Note that a resonance appears in all the off-mine measurements at approximately 900 Hz. This resonance can be attributed to the laser measurement apparatus, either from the laser itself, or from the tripod stand. In all measure-
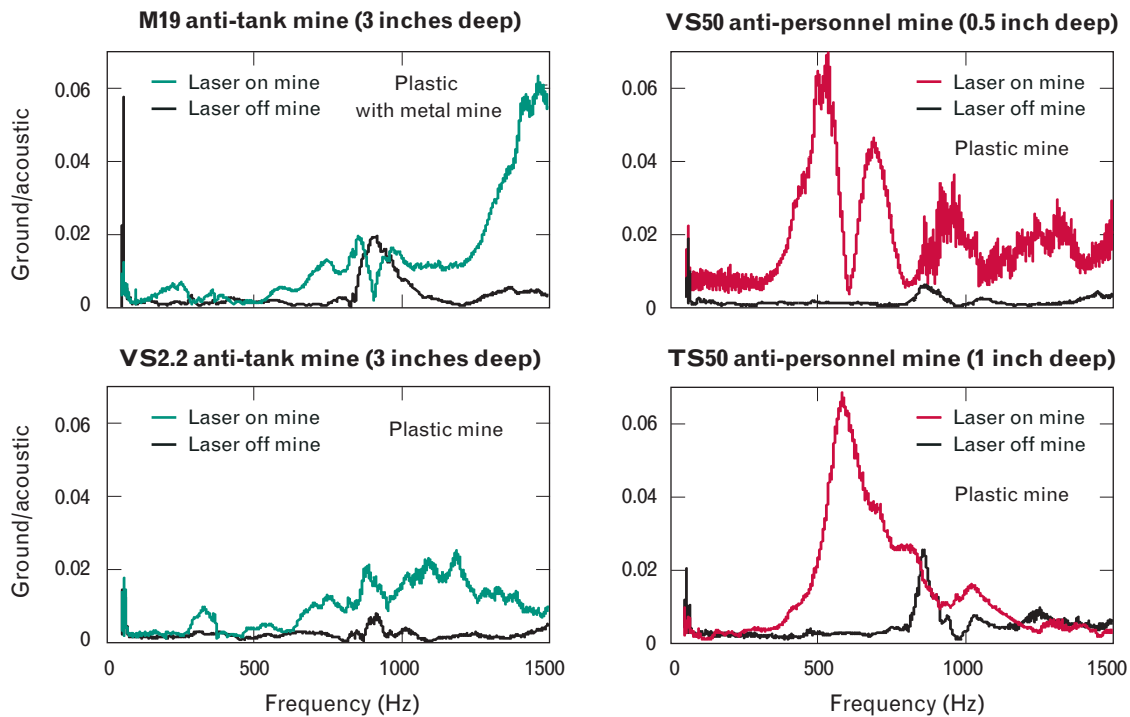
FIGURE 12. Low-frequency land-mine resonance measurements, using a subwoofer as the acoustic source, over a frequency range of 50 to 1500 Hz. Resonances from anti-tank mines, which are typically buried about three inches deep, are shown on the left. Resonances from anti-personnel mines, which are typically buried within a inch of the surface, are shown on the right. The signature amplitudes on the mine were clearly larger than those off the mine for all examples.

ments, the laser was not acoustically isolated from the subwoofer, and the tripod length varied slightly with setup over different mines.

The anti-tank and anti-personnel mines were also examined with the commercial PAA. The PAA produced a flat sound spectrum over the frequency band examined and did not require deconvolution processing. Signatures were observed for the anti-personnel mines (but not the anti-tank mines) at frequencies above 1000 Hz. Below 1000 Hz, the commercial PAA did not have ample acoustic power to sufficiently excite buried mines. This fall-off was attributed to the increasing power drop as the difference frequency became smaller. Figure 13 shows signatures on and off the anti-personnel mines. In both cases, resonances on the mines were observed over 2000 Hz, while no resonances were observed off the mines.

For all trials with this acoustic source, no signatures were observed for the anti-tank mines. We believe that the commercial PAA did not have enough acoustic power to penetrate the ground and produce a measur-

able response. This limitation is a topic of discussion in the next section.

Parametric Acoustic Array Power Analysis

The measured data show that the commercial PAA was able to excite buried anti-personnel mines and produce signatures that could be measured by the laser vibrometer at frequencies greater than 1000 Hz. However, the acoustic power of the commercial PAA was observed to drop with a decreasing difference frequency. Equation 5 shows that the difference-frequency pressure varies proportionately to the square of the difference frequency. Thus the pressure drops significantly as the difference frequency become smaller. For example, the acoustic power drops 40 dB when the difference frequency changes from 1000 to 100 Hz.

The sound pressure level (SPL) was measured with a microphone at the ground surface in the vicinity of the mine as a function of frequency for the PAA and the subwoofer. Figure 14 shows the measured SPL of both acoustic sources over the frequency range of our ex-
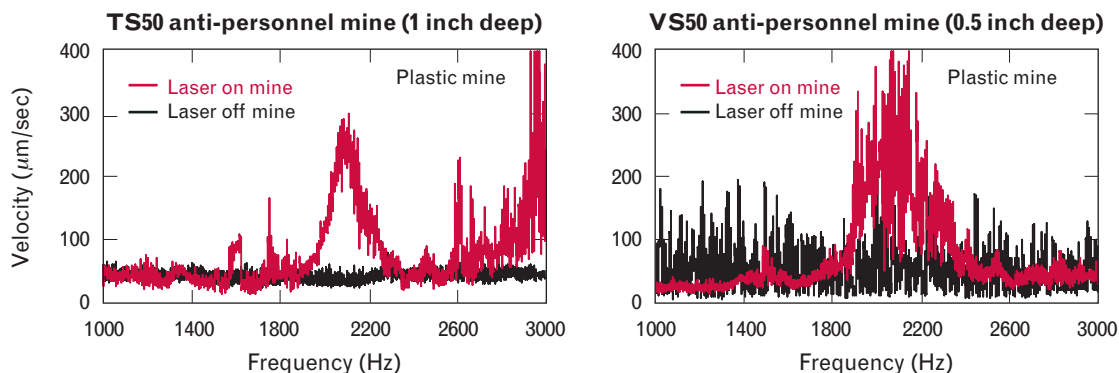
FIGURE 13. High-frequency anti-personnel land-mine resonance measurements, using the commercial PAA from 1000 to 3000 Hz. Resonances for these mines were clearly observed at frequencies over 2000 Hz. At frequencies below 1000 Hz, this acoustic source did not have sufficient power to excite any buried mines.

periments. A dashed line plotted at an SPL value of 77 dB (re 20 μPa) represents the observed acoustic power threshold that must be delivered to the ground surface above the mine to produce a sufficient vibration detectable by the PDV 100 laser vibrometer at three meters range. This threshold was determined by using acoustic sources independently over a frequency range of 50 to 3000 Hz and by observing a mine response with the laser vibrometer 3 dB above the laser noise floor. In these experiments, the threshold depended on the power of the commercial PDV 100 laser vibrometer and on the ground-glass spot applied to the measurement location used to enhance the signal-to-noise ratio. We anticipate that this threshold will vary if measurements are made with different laser vibrometers, with and without a dot of ground glass, and for different soil conditions.

The black curve shows the SPL generated by the commercial PAA at a distance of three meters. The curve appears relatively flat over frequency. This behavior is attributed to the commercial PAA power amplifier, which attempted to equalize the power level over a wide band of audible frequencies. Note that the Holosonics transducer array that forms the PAA was developed to produce quality sound with low distortion for music and other audio applications, while maintaining a relatively flat frequency response in the audio band. Below 800 Hz, the commercial PAA was unable to generate a mine response that was measurable with the laser vibrometer. Equation 5 predicts the SPL power decrease below 800 Hz, which rolls off at a rate of 12 dB per octave and is represented in the figure by the green dashed curve extensions.

The blue curve shows the SPL generated by the JBL subwoofer, which has a much higher power level than the commercial PAA at lower frequencies, especially below 1000 Hz, where Sabatier and others observed mine resonances [2–6]. We estimate that the subwoofer
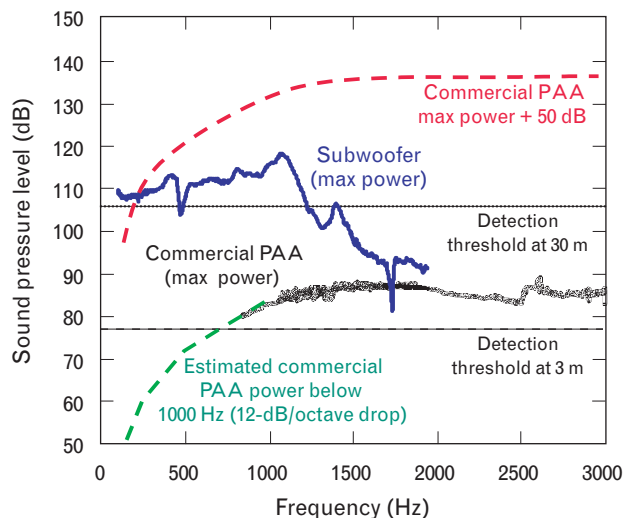
FIGURE 14. Power analysis of the PAA. The black dashes indicate the measured mine detection threshold at three meters. The dotted line indicates the power needed to excite mines at thirty meters. The black curve shows the sound pressure level (SPL) for the commercial PAA at maximum power three meters from the buried mine. This PAA has only marginal power for mine detection. The green dashes illustrate how quickly the power of the commercial PAA falls off at frequencies below 800 Hz. The blue curve shows the SPL for the JBL subwoofer at maximum power, which is higher at lower frequencies. The red dashes indicate the estimated 50-dB improvement in SPL that may be possible by redesigning the commercial PAA used in these experiments.

has marginal power to excite mines thirty meters away. Although these results offer some encouragement for improved land-mine detection, the JBL subwoofer still produces sound levels close to and above the threshold of pain, which is an important consideration in operator safety. At frequencies above 1000 Hz, the subwoofer power drops 20 to 30 dB and is comparable to that of the commercial PAA.

At three meters from the target, the commercial PAA appears to be marginal at best, even at frequencies above 1000 Hz. In its current configuration, the commercial PAA would be ineffective at thirty meters. We must remember, however, that the Holosonics commercial PAA was designed to produce sound for indoor audio use, with quality sound production well below the threshold of pain, and to maintain public user safety standards.

Designing the PAA for Land-Mine Detection

We have analyzed the capabilities of the commercial PAA, and we estimate that we can achieve up to a 50-dB gain in acoustic power by taking a different approach in the design of the PAA. The difference-frequency power of the PAA can be increased by choosing a lower pump frequency, increasing the input electrical power, improving the ultrasonic transducer efficiency, and increasing the size of the transducer array, compared to those features of the commercial PAA used in these tests. However, the selection of different PAA features requires net power tradeoffs, and thus an optimization design approach is appropriate. We developed a mathematical model to estimate the difference-frequency pressure profile over range for a PAA. Our model adds terms to the Westervelt equation to determine the PAA end-fire array length.

Tradeoffs between Characteristic Lengths

The difference-frequency pressure amplitude at range can be maximized by maximizing the length of the end-fire array established by the PAA. The resultant end-fire array length depends on three characteristic lengths, each controlled by the following three variables: pump wave attenuation, the PAA aperture, and acoustic saturation of the air. These terms are described in Equation 5, where the end-fire array length L is approximated by the minimum of the three characteristic

lengths, which were previously described in Equation 6. Figure 15 illustrates the three characteristic lengths and the resultant end-fire array length as a function of pump frequency.

The attenuation characteristic length A_L depends on the attenuation effects of air α with pump frequency ω, where

$$A_L = \frac{1}{\alpha(\omega)} \sim \frac{1}{\omega^2}.$$

Lower pump frequency waves attenuate less over range than higher frequency waves, and the attenuation characteristic length becomes smaller with increasing frequency, as illustrated by the green curve in Figure 15.

The aperture characteristic length R_L (the Rayleigh distance) of the PAA is a function of the end-fire array cross-sectional area S_0 and the pump frequency wavelength λ_i, where

$$R_L = \frac{\sqrt{2} S_0}{\lambda_i} \sim \omega.$$

The aperture characteristic length occurs at the range where all transducer element beams of the PAA combine to provide their maximum in-phase sum contribution to the sound beam. Beyond this length, the acoustic strength falls off from geometrical spreading. The
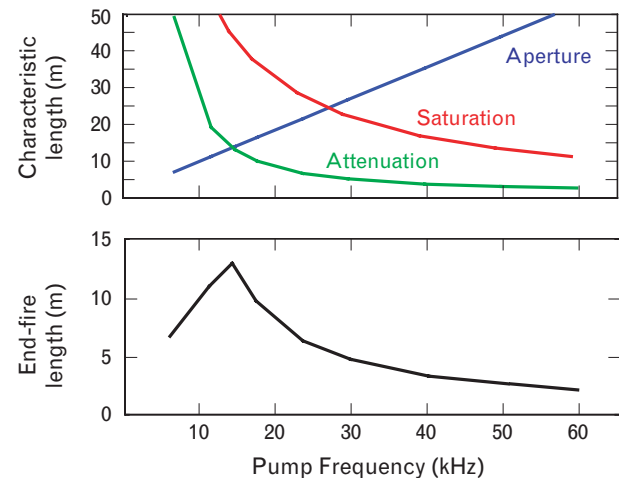
FIGURE 15. Three characteristic lengths of the PAA—attenuation, saturation, and aperture—as a function of pump frequency (top). The end-fire length of the PAA is the minimum of these three characteristic lengths (bottom). The PAA maximum difference-frequency pressure occurs at the end-fire array length.

transducer element beamwidth depends on frequency, where lower-frequency transducers have wider beam spreads than higher-frequency transducers and overlap with neighboring transducers at a closer range. Thus lower-frequency pumps have shorter aperture characteristic lengths than higher-frequency pumps, as illustrated by the blue curve in Figure 15.

The saturation characteristic length occurs at the range where the modulation envelope distortion that gives rise to the difference-frequency product cannot be increased with increased pump frequency power. Under these conditions, the pump wave has become a full shock wave (a sawtooth-shaped wave). Increasing the pump power beyond the saturation limit only results in additional harmonic frequency power with no net gain to the difference-frequency pressure. The saturation distance S_L, which can be described in terms of air and pump-wave properties, is given by

$$S_L = \frac{3}{\beta \varepsilon k} = \frac{3\rho c^3}{\beta P_i \omega_i} \sim \frac{1}{\omega}.$$

For a given pump pressure P_i, the saturation distance becomes shorter with an increase in the pump frequency ω_i, as illustrated by the red curve in Figure 15. The end-fire length at each pump frequency is thus the minimum of each of these three characteristic lengths, as shown by the black curve in Figure 15.

Figure 16 illustrates the saturation effect that occurs with increasing electrical input power to the PAA. The red curves show that the 60-kHz pump-frequency SPL flattens at electrical powers above 100 W. The corresponding difference-frequency SPL also flattens, indicating that additional electrical power results in no additional difference-frequency power. Lower pump frequencies at 15 kHz and 24 kHz are not significantly affected by saturation in the range of electrical power examined in these calculations.

End-Fire Array Length

The effective end-fire array length L results from the competing effects that define the characteristic lengths. Consequently, L is approximately the minimum of the three competing characteristic lengths—A_L, R_L, and S_L—and is shown by the black curve in the bottom plot of Figure 15. The end-fire length is small for low pump frequencies and increases to a maximum of fifteen me-
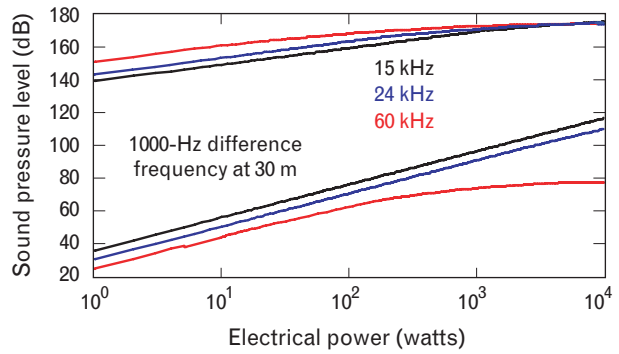

FIGURE 16. Effect of electrical power on pump power and difference-frequency power. At 60 kHz, the pump power and the difference-frequency power, shown in red, flatten out as electrical power increases, indicating that additional power saturates the PAA. Lower pump frequencies of 15 and 24 kHz, however, do not result in saturation.

ters, which corresponds to a pump frequency of 15 kHz for a PAA diameter of 24 inches. Below a pump frequency of 15 kHz, the PAA aperture controls the end-fire array length. Above 15 kHz, acoustic attenuation controls the end-fire array length, which falls off with increasing pump frequency.

Figure 17 gives the resultant difference-frequency pressure at 1000 Hz as a function of range for three different pump frequencies. The 15-kHz pump frequency produces the largest end-fire array length and difference-frequency pressure with range, compared to higher pump frequencies. Our model predicts that a pump frequency of 15 kHz provides a 26-dB gain in the difference-frequency power, while a 24-kHz pump exhibits a 21-dB improvement, compared to a 60-kHz pump frequency at a fifty-meter range.

Land-Mine PAA Optimization

Optimization of the end-fire array length can be accomplished by choosing a pump frequency, PAA cross-sectional area, and input electrical power to produce minimal characteristic lengths that are approximately the same for two or three competing effects. For example, the longest end-fire array length occurs for the 15-kHz pump frequency where the aperture and attenuation lengths coincide at the same range at fifteen meters, as depicted in Figure 15. In turn, the difference-frequency pressure amplitude increases to its maximum at fifteen meters, where it then falls off because of the effects of spherical spreading and attenuation.
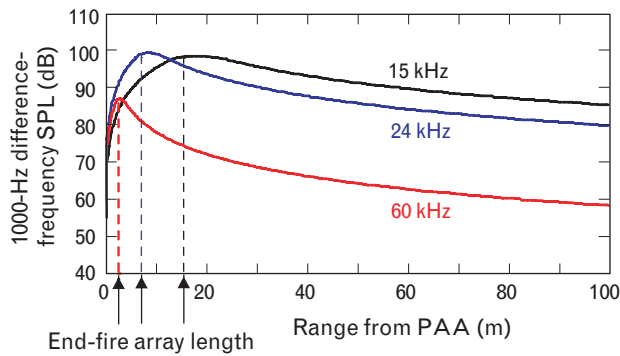
FIGURE 17. Difference-frequency SPL at 1000 Hz as a function of range for three different pump frequencies. The 15-kHz pump frequency produces the largest end-fire array length and the highest difference-frequency SPL for ranges beyond fifteen meters, but the pump frequency is audible and painful at these power levels. The 24-kHz pump frequency has a shorter end-fire array length but a difference-frequency SPL that is only 5 dB less for ranges greater than thirty meters. The 24-kHz pump frequency is inaudible and would have minimal effects on an operator.

Our approach is to design a land-mine PAA that emphasizes operational constraints. A 15-kHz pump frequency is in the audible frequency band and would have an SPL that approaches 160 to 170 dB, which would be dangerous to people without heavy-duty hearing protection. In contrast, a pump frequency in the ultrasonic band would have minimal effects to the operator and others in the vicinity of the equipment and mine. Choosing a pump frequency just above the audible band, such as 24 kHz, would result in a decrease in the end-fire array length, compared to the 15-kHz pump frequency. However, the net loss in the difference-frequency pressure power would be only 5 dB and would still provide ample power to excite a mine at a reasonable standoff range.

Figure 18 compares the performance of the commercial PAA with the performance that results from lowering the pump frequency and increasing the input electrical power. In the left plot, the difference-frequency pressure power is shown as a function of standoff range. The land-mine PAA used a 24-kHz pump frequency, twenty-four-inch-diameter end-fire array, and 1 kW of electrical power. We estimated that the Holosonics transducer array we purchased uses a 60-kHz pump frequency and operates at 200 W of electrical power. Modifying these parameters in the land-mine PAA pro-

vided a 27-dB gain in the difference-frequency power, compared to the power of the unmodified commercial PAA.

In the right plot of Figure 18, the difference-frequency power is plotted as a function of range and frequency for the land-mine PAA. The largest power is observed at a range between five and ten meters, which corresponds to the end-fire array length of a 24-kHz pump frequency. The output difference-frequency power falls from high frequency to low frequency and is proportional to the square of the difference frequency, as shown in Equation 5. These results indicate that the land-mine PAA can produce acceptable difference-frequency power levels above the mine detection threshold at frequencies approximately 500 Hz and higher, and at ranges up to thirty meters from the transducer array.

Additional difference-frequency power gains can be achieved by other modifications. The acoustic efficiency of the ultrasonic transducer can be improved, and we estimate a 10-to-20-dB gain over the commercial PAA. Increasing the land-mine PAA diameter from twenty-four to thirty-six inches can add an additional 4 dB. Summing the gains from each of these contributions—lowering the pump frequency, increasing electrical power, increasing the PAA end-fire array diameter, and enhancing ultrasonic transducer efficiency—could yield a net power gain approaching 50 dB over the current commercial PAA used in these tests.

PAA Application to Land Mines

Sabatier and others [2–6] and our own findings show that 100 to 300 Hz is a critical frequency band that can excite primary resonances in anti-tank mines. An acoustic frequency band from 200 to 600 Hz is typically used to excite the primary resonances in anti-personnel mines. We have observed additional resonances at frequencies above 1 kHz, but higher-frequency resonance magnitudes are significantly smaller than those of the primary resonances.

Our modeling results for a PAA show that it could be difficult to generate sufficient acoustic power at 100 Hz at safe standoff ranges. However, the PAA is likely to deliver the needed power at frequencies above 200 Hz, which would be useful in exciting resonances in anti-personnel mines and some anti-tank mines. Pulse-compression methods can be used to exploit higher-fre-
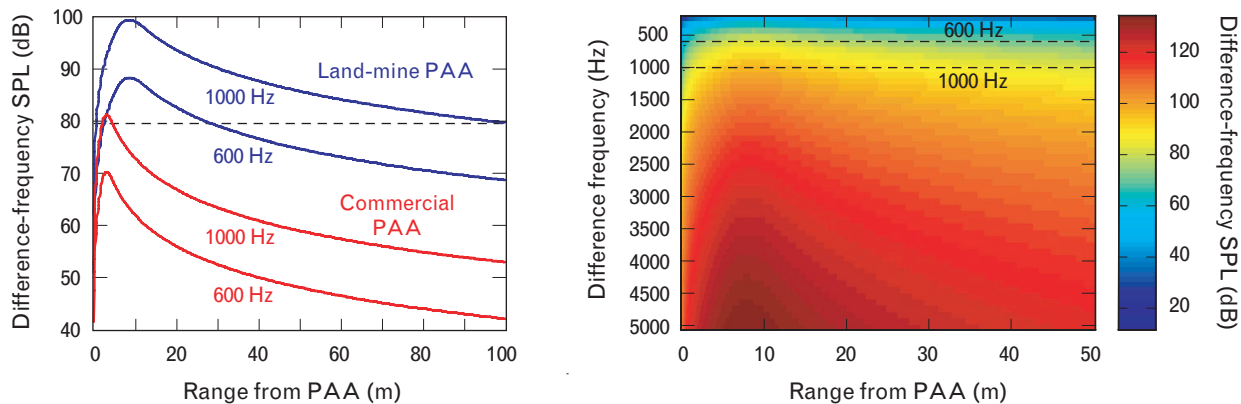
FIGURE 18. (left) Predicted performance of the land-mine PAA and the commercial PAA. The land-mine PAA simulates a 24-kHz pump frequency at 1 kW of electrical power for a 24-in transducer array. The commercial PAA simulates a 60-kHz pump at 200 W for a 24-in transducer array. The black dashed line shows acoustic threshold required for land-mine detection. Modifications to the land-mine PAA yield approximately a 30-dB power gain over the commercial PAA. (right) Simulated audible difference frequency for the land-mine PAA as a function of frequency and range. The dashed black lines indicate the location of the 600 Hz and 1000 Hz performance curves for the land-mine PAA.

quency backscatter returns for detection of both anti-tank and anti-personnel mines.

Several researchers observe their best detection results with loudspeakers and a laser vibrometer one meter directly above the mine. Xiang showed that the mine resonance amplitude depends on the laser vibrometer view angle relative to the ground where the mine resonance has a strong vertical component [2]. Resonance amplitudes are largest at a laser down-look angle (normal to the ground) over the mine, and they drop significantly at lower measurement angles. This result suggests that resonance detection by a forward-viewing laser vibrometer could be difficult.

The PAA has the ability to produce relatively higher power sound levels at frequencies above primary mine resonances. Despite the drop in higher-frequency mine resonance magnitudes, a large backscattered return off the mine is possible, as we observed in our land-mine facility experiments. The percentage of backscattered return is expected to increase as the acoustic and seismic wavelengths become smaller and approach the size of the mine. In addition, experimental results show that the backscattered return may not depend on viewing angle as strongly as the resonant returns, and thus may permit forward viewing with a laser vibrometer appropriate for standoff detection. N. Toksöz suggests that, at higher frequencies, slow seismic interface waves can be generated between the soil and mine [20]. These waves

can scatter and interfere with mines in their path and produce horizontal and vertical motion components at the ground surface. In some cases, strong horizontal motion can dominate the interface wave particle orbit.

Conclusions

The acoustic-to-seismic method shows promise as a useful tool to detect and map buried land mines. Several researchers have shown that the method can detect metal and nonmetallic mines with low false-alarm rates and low missed-target rates [2–9]. Even though work has been conducted to better understand the phenomenology of the technique, there is much to be done to develop a practical and operational method. System standoff range, operator safety, size, weight, speed of operation, and other parameters are key factors that need to be addressed. Developing a powerful, lightweight, and small acoustic source to excite mines in place would greatly advance this method. With this goal in mind, we believe the PAA is a worthwhile choice to test and evaluate.

We developed a proof-of-concept acoustic-laser system at Lincoln Laboratory to test the potential of using a PAA source to excite buried land mines for detection with a laser vibrometer. The system was built from off-the-shelf commercially available equipment. Unfortunately, much power is lost in the self-demodulation process from ultrasound to the audible frequency band

that excites mines. These experiments demonstrated, however, that a commercial parametric source could deliver sufficient power to excite buried anti-personnel mines. The source was unable to excite mines at lower frequencies typically examined by other researchers, but it had promising responses at higher frequencies. The reduced power at lower frequencies can be attributed to a predicted drop in power as the difference frequency becomes smaller in the self-demodulation process.

Although the commercial PAA produced only marginal power at close ranges to the mine, it is possible to redesign a parametric array to compensate for the losses in acoustic power observed in this experiment. By using a primary frequency just above the audible range, we can optimize the end-fire array length and design a customized PAA that is potentially suitable for standoff mine detection. The PAA also presents an opportunity to exploit frequencies higher than those currently being investigated by other researchers, and at ranges farther than those currently possible with conventional loudspeakers. The PAA has the added benefit of a directional beam-like sound pattern, which improves operator safety and comfort. Inside the beam the sound is painful, while off to the side but near the source the sidelobe leakage is minimal and well below the threshold of pain or discomfort. In addition, the weight and size of the PAA offer a clear advantage in portability over other acoustic source options.

Acknowledgments

REFERENCES

1. O.O. Bilukha, M. Brennan, and B.A. Woodruff, "Death and Injury from Landmines and Unexploded Ordnance in Afghanistan," *J. Am. Med. Assoc.* **290** (5), 2003, pp. 650–653.
2. N. Xiang and J.M. Sabatier, "An Experimental Study on Antipersonnel Landmine Detection Using Acoustic-to-Seismic Coupling," *J. Acoust. Soc. Am.* **113** (3), 2003, pp. 1333–1341.
3. J.M. Sabatier and N. Xiang, "An Investigation of Acoustic-to-Seismic Coupling to Detect Buried Antitank Landmines," *IEEE Trans. Geosci. Remote Sens.* **39** (6), 2001, pp. 1146–1154.
4. D.M. Donskoy, "Nonlinear Vibro-Acoustic Technique for Landmine Detection," *SPIE* **3392**, pt. 1, 1998, pp 211–217.
5. D.M. Donskoy, "Detection and Discrimination of Nonmetallic Landmines," *SPIE* **3710**, pt. 1, 1999, pp. 239–246.
6. M.S. Korman and J.M. Sabatier, "Nonlinear Acoustic Techniques for Landmine Detection: Experiments and Theory," *J. Acoust. Soc. Am.* **110** (5), pt. 2, 2000, 4pPA1, p. 2757.
7. W.R. Scott, Jr., J.S. Martin, and G.D. Larison, "Experimental Model for a Seismic Landmine Detection System," *IEEE Trans. Geosci. Remote Sens.* **39** (6), 2001, pp. 1155–1164.
8. W.R. Scott and J.S. Martin, "Experimental Investigation of the Acousto-Electromagnetic Sensor for Locating Land Mines," *SPIE* **3710**, pt. 1, 1999, pp. 204–214.
9. E.M. Rosen and K.D. Sherbondy, "Performance Assessment of Mine Detection Systems," *SPIE* **4038**, pt. 2, 2000, pp. 1225–1236.
10. R.E. Sheriff, ed., *Encyclopedic Dictionary of Exploration Geophysics,* 3rd ed. (Society of Exploration Geophysicists, Tulsa, Okla., 1991).
11. F.J. Pompei, "The Use of Airborne Ultrasonics for Generating Audible Sound Beams," *J. Audio Eng. Soc.* **47** (9), 1999, pp. 726–731.
12. M.A. Biot, "Theory of Propagation of Elastic Waves in a Fluid Saturated Porous Solid. I. Low-Frequency Range," *J. Acoust. Soc. Am* **28** (3), 1956, pp. 168-178; "Theory of Propagation of Elastic Waves in a Fluid Saturated Porous Solid. II. Higher Frequency Range," pp. 179–191.
13. Y.F. Sun, "Core-Log-Seismic Integration in Hemipelagic Marine Sediments on the Eastern Flank of the Juan de Fuca Ridge," *Proc. Ocean Drilling Program, Scientific Results* **168**, A.T. Fisher, E.E. Davis, and C. Escutia, eds. (College Station, Tex., Ocean Drilling Program, 2000), pp. 21–35.
14. J. Sabatier, "Acoustic-to-Seismic Coupling and the Humanitarian Demining Problem," <www.censsis.neu.edu/documents/ASCHD.pdf>.
15. H.O. Berktay, "Possible Exploitation of Non-Linear Acoustics in Underwater Transmitting Applications," *J. Sound Vib.* **2** (4), 1965, pp. 435–461.
16. M.B. Bennett and D.T. Blackstock, "Parametric Array in Air," *J. Acoust. Soc. Am.* **57** (3), pp. 562–568.
17. M. Yoneyama, J.-I. Fujimoto, Y. Kawamo, and S. Sasabe, "The Audio Spotlight: An Application of Nonlinear Interaction of Sound Waves to a New Type of Loudspeaker Design," *J. Acoust. Soc. Am.* **73** (5), 1983, pp. 1532–1536.
18. P.J. Westervelt, "Parametric Acoustic Array," *J. Acoust. Soc. Am.* **35** (4), 1963, pp. 535–537.
19. K.D. Rolt, "A Dissipative Wave Packet Approach for Unified Nonlinear Acoustics," Ph.D. thesis (Ocean Engineering, MIT, Cambridge, Mass., 1994).
20. Communications with N. Toksöz and D. Burns, MIT Earth Resources Laboratory; Earth, Atmospheric, and Planetary Sciences Department (April 2004).

ROBERT W. HAUPT
is a staff member in the Advanced System Concepts group. He joined Lincoln Laboratory in 1996. His interests are in seismic and electromagnetic wave propagation in complex media, field-scale experimentation, and numerical simulation. His research at the Laboratory has focused on developing seismic and acoustic methods to characterize underground facilities. Some of his major contributions have been in seismic shear-wave data acquisition and in processing techniques used to image tunnels. He is currently researching acoustic-laser methods to detect buried land mines and improvised explosive devices. He has also performed systems analysis for air-defense systems and air-vehicle survivability. He received a B.S. degree in physics and a B.S. degree in meteorology from S.U.N.Y. Oswego, an M.S. degree in geophysics from Penn State University, and an M.S. degree in mechanical engineering from Dartmouth. He previously worked as an exploration geophysicist in the oil and minerals industry in the Rocky Mountains and western Canada, where he experienced being "treed" by bears, and where he witnessed a helicopter crash from the passenger seat. His less dangerous interests include raising four kids, playing the saxophone, and woodworking.

KENNETH D. ROLT
is a staff member in the Advanced Sensor Techniques group, where he works in passive and active sonar processing and automation. He joined Lincoln Laboratory in 2000 after working at Lockheed Sanders (now BAE) and Raytheon. In addition to sonar, his research interests include target analysis, wave propagation and scattering, antenna design, volcanology, and automotive engineering. He is a member of the Acoustical Society of America, a reviewer for the Society of Automotive Engineers, a member of the Westford Police Amateur Radio Team, a radio amateur (call sign KB1FFM), a Westford-based member of the Lowell Emergency CERT team, and a Den leader and Cub Master for Pack 99 in Westford. He has a B.S. degree in mechanical engineering and a B.A. degree in journalism from the University of Massachusetts, Amherst, and an S.M. degree in ocean engineering and a Ph.D. degree in acoustics from MIT.